nature water

Article

https://doi.org/10.1038/s44221-023-00033-4

Impact of sewer biofilms on fate of SARS-CoV-2 RNA and wastewater surveillance

Received: 31 May 2022

Accepted: 11 January 2023

Published online: 9 February 2023

Check for updates

Jiaying Li[1] ✉, Warish Ahmed[2], Suzanne Metcalfe[2], Wendy J. M. Smith[2], Phil M. Choi[3], Greg Jackson[3], Xiaotong Cen[4], Min Zheng[4], Stuart L. Simpson[5], Kevin V. Thomas[1], Jochen F. Mueller[1] & Phong K. Thai[1]

With wastewater surveillance being implemented worldwide to aid in managing coronavirus disease 2019 (COVID-19), there is a need to understand the fate of severe acute respiratory syndrome coronavirus 2 (SARS-CoV-2) in sewer systems. Here we employed a sewer reactor to investigate sorption, decay and persistence of SARS-CoV-2 RNA in sewers. RNA concentrations were positively correlated between wastewater liquid and suspended solids, and between wastewater mixture and sewer biofilms. We identified two roles of biofilms in mediating the fate of SARS-CoV-2 RNA. Firstly, biofilms could affect RNA in-sewer stability. This impact could be limited in typical sewer systems with high COVID-19 prevalence, as estimated RNA loss was relatively small. However, in low-case settings, in-sewer RNA decay could affect detectability and precision of analysis, particularly over long hydraulic retention times before sample collection. The second role of biofilms is a reservoir for accumulating, retaining and distributing SARS-CoV-2 RNA under hydraulic changes, which could lead to prolonged virus presence and affect wastewater surveillance interpretation.

Wastewater monitoring for coronavirus disease 2019 (COVID-19) is an effective and minimally invasive approach for detecting and quantifying gene fragments (RNA) of severe acute respiratory syndrome coronavirus 2 (SARS-CoV-2) from communities. Wastewater surveillance has demonstrated ability in early warning, estimation of COVID-19 prevalence and identification of new variants[1–3]. Wastewater surveillance can be more practical and economical (screening at the population level) than mass swab testing of individuals. Consequently, wastewater testing of SARS-CoV-2 has been implemented worldwide to complement local and global public health surveillance systems[1,4,5]. However, many uncertainties currently exist, notably in regard to dynamic viral shedding rate, virus recovery from wastewater matrices and the fate of SARS-CoV-2 shed from infected persons to wastewater collection points[6,7]. So far, the fate of SARS-CoV-2 RNA in real sewer networks has not been well documented. This could affect the credibility (of both detection and quantitation) of wastewater results obtained at wastewater treatment plants (WWTPs).

Previous studies have suggested that sewer biofilms could play important roles in mediating the fate of viruses, as a natural reservoir accumulating viruses and/or as a facilitator of decay or inactivation of viruses by microbial processes. Stability of viral concentrations in wastewater is a dynamic equilibrium between attachment and detachment processes[8]. The accumulation of viruses (for example, enterovirus, norovirus and F-specific RNA phages) in biofilms has been observed in water and wastewater systems[9–13], where biofilms provide binding sites for viruses and shelter them from inactivation or degradation[14]. Studies have reported longer persistence of viruses when associated with biofilms or solids compared with the free-flowing viral particles in water[8,15]. Additionally, the detachment of virus from biofilms and the erosion and sloughing of virus-bound biofilms were observed under hydraulic changes[12,13]. The retention of viruses

[1]Queensland Alliance for Environmental Health Sciences (QAEHS), The University of Queensland, Brisbane, Queensland, Australia. [2]CSIRO Land and Water, Ecosciences Precinct, Brisbane, Queensland, Australia. [3]Water Unit, Health Protection Branch, Queensland Public Health and Scientific Services, Queensland Health, Brisbane, Queensland, Australia. [4]Australian Centre for Water and Environmental Biotechnology, The University of Queensland, Brisbane, Queensland, Australia. [5]CSIRO Land and Water, Lucas Heights, Sydney, New South Wales, Australia. ✉e-mail: jiaying.li@uq.edu.au

https://doi.org/10.1038/s44221-023-00033-4

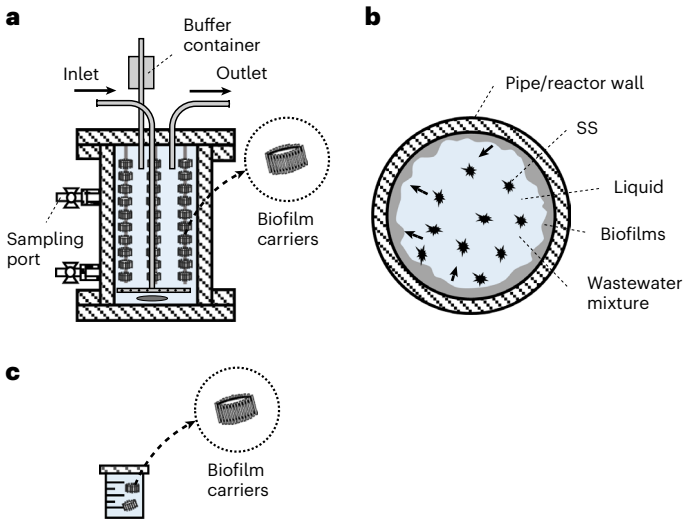

Fig. 1 | Sewer biofilm reactor and testing chamber. a, The Reactor used in this study. **b**, Cross-section of the Reactor with different sewage compartments, namely wastewater mixture comprising liquid and suspended solids, and biofilms growing on inner surface of Reactor wall. **c**, The Chamber used to create the outside-reactor condition containing wastewater mixture and individual biofilm carriers transferred from the Reactor before each experiment.

in biofilms could lead to extended virus dispersion and circulation, posing a risk of contamination or infection from some waterborne diseases[9,11,12]. Additionally, biofilms may facilitate decay of the virus and/or its genetic fragments in sewers. Viable viruses typically decay rapidly in bulk wastewater, with an estimated T_{90} of 1.6–2.1 days for infectious SARS-CoV-2 (ref. [16]) and 2.7–6.3 h for infectious coronavirus surrogates[17] at room temperature. Biofilms could further accelerate virus decay and inactivation, which shortened the T_{90} of infectious coronavirus surrogates to 0.86–1.72 h (ref. [17]). In contrast to viable virus, SARS-CoV-2 RNA was persistent with a longer range of T_{90} from 0.8 to 26 days in untreated wastewater[2,16,18]. It was suggested that SARS-CoV-2 RNA could remain stable over up to 5 h when monitoring temporal changes in RNA along a real sewer pipe[19].

The issues related to virus presence and longevity in sewers are important to wastewater surveillance, particularly in low infection case settings and at the end of local epidemics, where virus occurrence and concentrations are disproportionately susceptible to fluctuation. To address the current knowledge gap in the fate of SARS-CoV-2 in sewers, this study aimed to provide three forms of essential information, namely the sorption coefficients of SARS-CoV-2 RNA to solid compartments in sewers, the stability of SARS-CoV-2 RNA in sewers under the influence of biofilms and the role of biofilms in entrapping and further distributing viral RNA fragments with wastewater flushes. In this Article, we systematically investigated the behaviour of SARS-CoV-2 RNA using a bench-scale sewer biofilm reactor (hereinafter referred to as the Reactor), capable of cultivating biofilms and simulating realistic sewer conditions. This study adds new knowledge on the fate of SARS-CoV-2 RNA in sewer systems and advances wastewater surveillance efforts in qualitative and (semi)quantitative assessments of COVID-19 prevalence in the population, which is increasingly relied on with the reduction of individual clinical testing.

Sorption of SARS-CoV-2 RNA to suspended solid and biofilms

The Reactor employed in this study represented the realistic conditions of a sewer pipe section, which contained different sewage compartments, including the bulk wastewater (750 ml) as a mixture of liquid and suspended solids (SS), and the intact biofilm system growing on inner surface of the Reactor and on removable biofilm carriers installed in the Reactor (Fig. 1a,b). In addition, the testing chambers (referred to as the Chambers) were employed for the sorption experiment. Each Chamber contained 50 ml of wastewater with one to two biofilm carriers transferred from the Reactor right before each batch test (Fig. 1c). The main difference between the Reactor and Chambers was the abundance of biofilms, which were quantifiable using the ratio of biofilm surface area to wastewater volume (A/V: Reactor 63 $m^2\ m^{-3}$, Chamber 5–10 $m^2\ m^{-3}$).

The addition of known numbers of SARS-CoV-2 RNA gene copies (GC) into the Reactor and Chambers generated the sewage conditions with a range of environmentally relevant RNA concentrations from low to high levels (statistically significantly different, $P < 0.05$; for values, see Supplementary Table 1). All collected samples from various sewage compartments in the Reactor and Chambers had detected and quantifiable RNA levels. The viral RNA concentrations in wastewater mixture (C_{ww}) of the Reactor and Chambers ranged from 18.0 to 7.90×10^5 GC ml^{-1}. After centrifugation of the wastewater mixture, viral RNA concentrations ranged from 17.8 to 6.18×10^5 GC ml^{-1} in the liquid phase (C_l) and 3.99×10^3 to 4.18×10^7 GC g^{-1} in the paired SS phase (C_{ss}). The viral RNA concentration range in biofilm samples (C_{bio}) was 43.7 to 1.72×10^5 GC cm^{-2}. The number of RNA GC distributed among separate phases was determined by converting viral concentration to the volume, mass or surface area of each corresponding matrix (Supplementary Table 1). It was found that the proportion of RNA GC in individual sewer compartments was different between the conditions provided by the Chambers and the Reactor (Supplementary Table 1). In the Chambers with the presence of individual biofilm carrier(s), the proportion of RNA was higher in the liquid (73.3 ± 8.3%) than in SS (17.3 ± 7.5%) and biofilms (9.8 ± 13.2%), showing significant difference between liquid and SS ($P = 0.0001$) and between wastewater mixture and biofilms ($P = 0.002$). In the Reactor with a high abundance of biofilms, the intact biofilm system was found to be the major reservoir of SARS-CoV-2 RNA (78.0 ± 22.2%) compared with the GC in wastewater (22.0 ± 22.2%) ($P = 0.01$). For the virus signature in wastewater of the Reactor, there were similar proportions between liquid (14.6 ± 14.6%) and SS (19.3 ± 5.7%) ($P = 0.67$).

The concentrations of SARS-CoV-2 RNA in the solid compartments (SS and biofilms) increased with the higher SARS-CoV-2 RNA concentrations in the aqueous compartments (wastewater liquid and mixture) (Fig. 2a). Positive correlations were determined between C_{ss} and C_l (Spearman $r = 0.80$, $P = 0.005$) and between C_{bio} and C_{ww} (Spearman $r = 0.76$, $P = 0.003$). The estimated sorption coefficients (K_d) are reported in Table 1 with comparisons shown in Fig. 1b. The estimated K_{d_ss} for the adsorption of RNA onto SS had a median of 117 ml g^{-1} considering all datasets, wherein K_{d_ss} determined inside the Reactor (median 372 ml g^{-1}) was significantly higher than K_{d_ss} determined in Chambers (median 66 ml g^{-1}) ($P = 0.006$). The estimated K_{d_bio} for the adsorption of RNA onto biofilms had a median of 3.1 ml cm^{-2} taking all datasets into account, wherein K_{d_bio} determined inside the Reactor (median 12 ml cm^{-2}) was significantly higher than K_{d_bio} in Chambers (0.22 ml cm^{-2}) ($P = 0.01$).

Decay of SARS-CoV-2 RNA in sewers with biofilms

Decreases in SARS-CoV-2 RNA concentrations were observed in the Reactor during 24 h hydraulic retention times (HRTs), with various transformation patterns shown in different sewage compartments (Fig. 3a). With an initial concentration of 90–416 GC ml^{-1} for endogenous SARS-CoV-2 RNA in wastewater, C_{ww} decreased by 41–82% over 24 h compared with initial concentrations (with a significant decreasing trend, $P = 0.001$). Showing similar transformation patterns, the first-order decay rates for SARS-CoV-2 RNA (k_1; for equation, see Methods) in liquids (C_l) and wastewater mixtures (C_{ww}) were estimated as 0.050 h^{-1} and 0.045 h^{-1}, respectively, with corresponding half-lives of 14 and 16 h, and T_{90} of 46 and 52 h (Table 2). In contrast to the decrease in the

https://doi.org/10.1038/s44221-023-00033-4

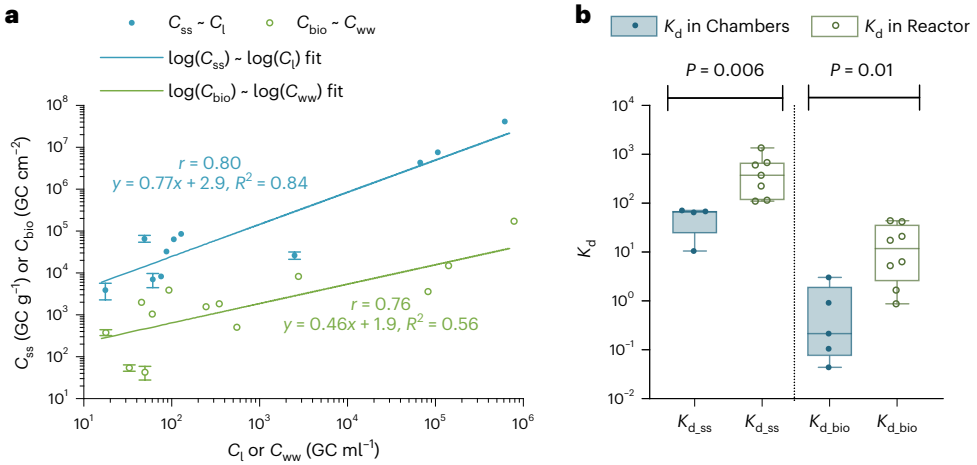

Fig. 2 | Sorption of SARS-CoV-2 RNA to suspended solids and sewer biofilms. **a**, Relationship of SARS-CoV-2 RNA concentrations between SS and wastewater liquid C_{ss} ~ C_l (blue filled circles. n = 11 independent replicates. Spearman correlation coefficient r = 0.80) and relationship of RNA concentrations between sewer biofilms and wastewater mixture C_{bio} ~ C_{ww} (green unfilled circles,; n = 13 independent replicates, Spearman correlation coefficient r = 0.76) at equilibrium. Data are presented as mean values with standard deviation (s.d.). Log transformation data are fitted using linear regression in GraphPad Prism 8. **b**, Estimated sorption coefficients of SARS-CoV-2 RNA onto SS (K_{d_ss}, ml g^{-1}) and onto biofilms (K_{d_bio}, ml cm^{-2}) in sewer matrices of Chambers (blue filled circles, K_{d_ss} n = 4, K_{d_bio} n = 5, independent samples) and Reactor (green unfilled circles; K_{d_ss} n = 7, K_{d_bio} n = 8, independent samples). Sorption coefficients determined between Chambers and the Reactor showed significant difference, K_{d_ss} P = 0.006 and K_{d_bio} P = 0.01 (two-sided Mann–Whitney test). The box plots display median and extend from the 25th to 75th percentiles, with the upper whiskers extending to the 90th percentile and the lower whiskers extending to the 10th percentile. Data are provided in source data.

Table 1 | Sorption coefficient (K_d) of SARS-CoV-2 RNA to wastewater suspended solids and sewer biofilms estimated in this study

Sorption coefficient	K_{d_ss}=C_{ss}/C_l (ml g^{-1})	K_{d_bio}=C_{bio}/C_{ww} (ml cm^{-2})
Overall		
Median	117	3.1
Mean (s.d.[a])	334 (407)	11.1 (15.8)
Test chamber		
Median	66.2	0.22
Mean (s.d.[a])	53.5 (28.6)	0.87 (1.3)
Minimum and maximum	10.7–70.9	0.04–3.1
Sewer biofilm reactor		
Median	372	12.0
Mean (s.d.[a])	494 (440)	17.4 (17.5)
Minimum and maximum	112–1,353	0.88–44.2
K_d comparison between Chamber and Reactor (two-sided Mann–Whitney test)	Significantly different, P=0.006	Significantly different, P=0.01

[a]Standard deviation.

aqueous phases, SARS-CoV-2 RNA concentrations were relatively steady in biofilms (C_{bio}), being within ±20% over 24 h (non-significant change, P = 0.79). Viral RNA concentrations in SS (C_{ss}) showed either partial increases or decreases over the course of time, but without significant change compared with initial concentrations (P = 0.89). During the study, strong biological activities were detected in the Reactor indicated by a high sulfide production rate of 2.60 ± 0.53 g S^{-1} m^{-2} day^{-1}, which was similar to the typical level in real sewer pipes[20]. The monitoring of rhodamine (a water tracer used to indicate hydraulic dynamics) during the experiment showed limited change in rhodamine signals (within ±10%), suggesting the Reactor was under a steady hydraulic condition without wastewater input or output.

The total numbers of SARS-CoV-2 RNA GC in the Reactor decreased by 23–69% over 24 h HRTs (with a non-significant temporal trend, P = 0.18) (Fig. 3b). The numbers of RNA GC distributed in wastewater mixture (N_{ww} 2.3 × 10^4 to 3.1 × 10^5 GC) and biofilms (N_{bio} 2.1 × 10^4 to 8.6 × 10^5 GC) were at the same orders of magnitude. The decrease in N_{ww} over time was significant (P = 0.001), which was fitted by a first-order kinetics with an estimated decay rate (k_2) of 0.05 h^{-1}, a half-life of 14 h and T_{90} of 45 h (Table 2). Decrease of N_l showed a similar pattern as N_{ww} with a first-order decay rate of 0.06 h^{-1}. N_{ss} decreased by 32–42% after 24 h compared with the initial, showing a significant decreasing trend (P = 0.04). The change in N_{ss} was found to be related to the decreasing SS concentrations (due to SS hydrolysis and settlement) over HRTs in the Reactor. The change of N_{bio} was relatively small, varying within ±25% over 24 h (P > 0.05). Consequently, the decrease of total GC (N_{total}) in the Reactor was a combined result of the changes in both wastewater and biofilm phases, which was mainly driven by RNA decay in wastewater. A first-order decay rate k_2 of 0.03 h^{-1} was estimated for the change of N_{total}, resulting in a half-life of 27 h and T_{90} of 90 h.

Persistence of SARS-CoV-2 RNA under hydraulic changes

Under the impact of wastewater exchanges, SARS-CoV-2 RNA exhibited stronger persistence compared with the rapid dissipation of rhodamine signals in the Reactor (Fig. 4). The intermittent wastewater exchanges (with SARS-CoV-2-negative wastewater) were created to simulate the plug-flow condition in real rising main pipes. The first exchange event flushed the majority of original SARS-CoV-2-positive wastewater out of the Reactor, as indicated by the decrease in rhodamine signal in wastewater by 64 ± 16%. In contrast, an evident spike of SARS-CoV-2 was detected in the first effluent from the Reactor, of which the number of GC was 159–225% of the initial N_{ww} in the Reactor before the first wastewater exchange event. During the following exchange events, rhodamine signals in wastewater were reduced to 18 ± 6%, 8 ± 4% and 4 ± 3% after the second, third and fourth flushes, respectively. The decreases

https://doi.org/10.1038/s44221-023-00033-4

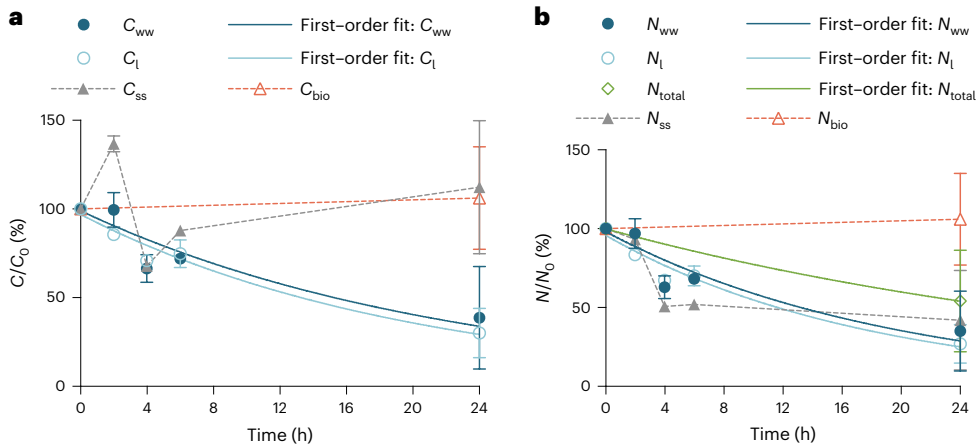

Fig. 3 | Decay of SARS-CoV-2 RNA in sewers. a, Changes of SARS-CoV-2 RNA concentrations in samples collected from the Reactor, including wastewater mixture (C_{ww} $n = 11$, independent samples; dark-blue filled circles), liquid (C_l $n = 9$, independent samples; light-blue unfilled circles), SS (C_{ss} $n = 8$, independent samples; grey filled triangles) and biofilm (C_{bio} $n = 4$, independent samples; orange unfilled triangles) phases. Data are presented as mean values with s.d. Transformation trends of C_{ww} and C_l are fitted with first-order kinetics using equation (3). **b**, Changes of viral GC numbers in different sewer compartments of the Reactor, including wastewater mixture (N_{ww} $n = 11$, independent samples; dark-blue filled circles), liquid (N_l $n = 9$, independent samples; light-blue unfilled circles), SS (N_{ss} $n = 8$, independent samples; grey filled triangles), biofilm (N_{bio} $n = 4$, independent samples; orange unfilled triangles) phases and total GC number in the Reactor (N_{total} $n = 4$, independent samples; green unfilled diamonds). Data are presented as mean values with s.d. Transformation trends of N_{ww}, N_l and N_{total} are fitted with first-order kinetics during the 24 h testing period using equation (4). Data are provided in source data.

of N_{ww} in effluents were slower than the concurrent rhodamine dissipation, with N_{ww} at 77 ± 40% and 48 ± 4% of the initial GC after the second flush and the third flush, respectively. After the fourth exchange event, N_{ww} in the effluent was reduced to 44% of initial GC in one batch test; in another batch test, however, a large increase in virus GC was observed in the effluent, which was 128% of the initial GC and 323% of N_{ww} in the Reactor before the fourth exchange event.

It was observed that SARS-CoV-2 RNA persisted longer in biofilms than rhodamine water tracer in the wastewater phase of the Reactor when undergoing hydraulic changes. After three wastewater exchange events with virus-free wastewater, 51–68% of the initial N_{bio} remained in the Reactor (non-significant change, $P = 0.16$), in contrast to the virtually complete dissipation of rhodamine signals in wastewater. During the experiments, biofilms harboured approximately 81–97% of total GC (N_{bio} 5.0×10^5 to 1.9×10^6 GC), compared with RNA present in wastewater mixture (N_{ww} 2.9×10^4 to 2.6×10^5 GC). The total RNA GC in the Reactor (N_{total}), as a combination of RNA in both wastewater and biofilm phases, showed a moderate decrease during wastewater exchange events. The ratio of N_{total} at 0 h (before the first flush) to 6 h (before the fourth flush) suggested that 56 ± 6% of initial GC remained in the Reactor after three flushes, while more than 95% of the original wastewater had been replaced by new wastewater (free of SARS-CoV-2 RNA) as indicated by the loss of rhodamine signals.

Discussion

In this study, we identified two roles of biofilms in mediating the fate of SARS-CoV-2 RNA in sewers: firstly, biofilms could facilitate RNA biodegradation, which might cause RNA signal loss over long HRTs; secondly, biofilms form a reservoir for viral RNA, protecting virus fragments from being washed off during hydraulic changes, and subsequently releasing RNA fragments back to surrounding wastewater. This suggested that the fate of SARS-CoV-2 RNA in sewers was a dynamic equilibrium between adsorption, decay, desorption and detachment of RNA associated with biofilms, similar to findings of previous studies for other bacterial and viral indicators[8,21]. According to observations in this study, the adsorption and accumulation of SARS-CoV-2 RNA onto biofilms played a dominant role, particularly with respect to degradation, leading to the persistence of RNA in a sewer section after several wastewater replacements. This indicates that after SARS-CoV-2 has been shed from infected persons into sewer systems, multiple in-sewer factors including hydraulic dilution, viral degradation, accumulation onto biofilms and release of biofilm-associated virus particles will jointly affect RNA occurrence in WWTP influents.

Results of the sorption experiments demonstrated the accumulation of SARS-CoV-2 RNA onto solids and biofilms in sewers, with increasing adsorption tendency under the biofilm-rich condition, which offered more niches and sorption sites for virus binding. The consistent mixing in the Reactor could also facilitate RNA partitioning to solid phases, compared with that in the Chambers under a static condition. There have been a few investigations about sorption behaviour of SARS-CoV-2 RNA in wastewater matrices; however, the role of sewer biofilm was not mentioned. Li et al. (2021) found that the majority of SARS-CoV-2 RNA was partitioned to solids (82–93%) in wastewater with a high solid–liquid ratio of $10^{3.6}$–$10^{4.3}$ ml g^{-1} (ref. [22]). Graham et al. (2021) found that virus concentrations in primary settled sludge were ~100 to ~1,000 times higher than that in wastewater influent, leading to a ratio of 350–3,100 ml g^{-1} (ref. [23]). The opposite observation was reported where 91% of SARS-CoV-2 RNA was present in the liquid phase compared with RNA adsorbed on wastewater solids[2]. In addition to wastewater solids, sewer biofilm is an essential compartment of sewer systems, performing potentially specific interactions with SARS-CoV-2. Our study determined that the majority of SARS-CoV-2 RNA GC was accumulated in abundant biofilms in a sewer section. However, several factors need to be considered before transferring the results of this study to real applications, including biofilm properties (for example, A/V ratios) and catchment conditions (for example, HRTs, wet weather flows and disease prevalence). In this study, the detection of SARS-CoV-2 RNA in biofilms was normalized to biofilm surface areas, which were quantifiable for biofilms on carriers and the reactor's inner surface. However, virus may diffuse into biofilm deeper layers, particularly when biofilms had been exposed to SARS-CoV-2 for a long period. The unknown saturation of SARS-CoV-2 in biofilms and the dynamic equilibrium impeded attempts at calculating the mass balance of SARS-CoV-2 RNA GC or examining its complete removal from the Reactor.

Understanding the fate of SARS-CoV-2 RNA in sewer systems is crucial to interpretating wastewater surveillance results, especially

https://doi.org/10.1038/s44221-023-00033-4

Table 2 | Decay rate (*k*) of SARS-CoV-2 RNA concentrations and GC numbers estimated in this study

Decay rate	$C = C_0 \times e^{-k_1 \times t}$		$N = N_0 \times e^{-k_2 \times t}$
Wastewater liquid (C_l)		**Wastewater mixture (N_{ww})**	
k_1 (h^{-1}) mean (s.d.)	0.050 (0.0071)	k_2 (h^{-1}) mean (s.d.)	0.051 (0.014)
k_1 (95% confidence interval)	(0.035, 0.070)	k_2 (95% confidence interval)	(0.025, 0.099)
R^2	0.94	R^2	0.77
Half-life, T_{90} (h)	13.9, 46.2	Half-life, T_{90} (h)	13.6, 45.2
Wastewater mixture (C_{ww})		Total GC (N_{total})	
k_1 (h^{-1}) mean (s.d.)	0.045 (0.013)	k_2 (h^{-1}) mean (s.d.)	0.026 (0.014)
k_1 (95% confidence interval)	(0.020, 0.086)	k_2 (95% confidence interval)	(0.012, 0.039)
R^2	0.73	R^2	0.67
Half-life, T_{90} (h)	15.5, 51.6	Half-life, T_{90} (h)	27.1, 90.0
Comparison of fits[a]	First order is preferred[b]	Comparison of fits	First order is preferred[c]

[a]Comparison of fits between four models using extra sum-of-squares *F* test and Akaike's corrected Information Criterion (AICc). Model 1—first-order kinetics, model 2—linear regression, model 3—two-phase decay, model 4—second-order kinetics. Null hypothesis: first-order kinetics (model 1) is preferred. [b]Comparison of fits for C_l transformation (n=9): model 1 is preferred. For Model 1 versus 2, 3, 4, degrees of freedom (DF): 7 versus 7, 5, 6; AICc: probability that model 1 is correct—78.5%, -, 97.4%; R^2: 0.94 versus 0.91, 0.94, 0.93. Comparison of fits for C_{ww} transformation (n=11): model 1 is preferred. For Model 1 versus 2, 3, 4, DF: 9 versus 9, 7, 8; *F*: -, 0.44, 1.16; AICc: probability that model 1 is correct—68.0%, 99.7%, 86.7%; R^2: 0.73 versus 0.70, 0.76, 0.77. [c]Comparison of fits for N_{ww} transformation (n=11): model 1 is preferred. For Model 1 versus 2, 3, 4, DF: 9 versus 9, 7, 8; *F*: -, 0.68, 1.79; AICc: probability that model 1 is correct—75.0%, 99.5%, 81.9%; R^2: 0.77 versus 0.72, 0.81, 0.81. Comparison of fits for N_{total} transformation (n=4): model 1 is preferred. For Model 1 versus 2, 3, 4, DF: 2 versus 2, -, 1; R^2: 0.67 versus 0.67, -, 0.67.

when wastewater-based approaches are increasingly relied on to monitor and compare trends in COVID-19 prevalence in communities with diminished individual clinical testing. This study demonstrated that biofilms played different roles under varying hydraulic conditions and could cause specific impacts on wastewater result interpretation. The in-sewer decay rate of SARS-CoV-2 RNA determined in this study (0.05 h^{-1}) was similar to the results of Weidhaas et al.[2] with first-order decay rates of 0.09–0.12 h^{-1} for SARS-CoV-2 RNA in wastewater, and relatively higher than decay rates of 0.004–0.03 h^{-1} for SARS-CoV-2 RNA reported in Bivins et al.[16] and 0.005–0.008 h^{-1} for gamma-irradiated SARS-CoV-2 RNA estimated by Ahmed et al.[18] in wastewater (a summary of decay rates is provided in Supplementary Table 2). The in-sewer decay rate of SARS-CoV-2 RNA is crucial to the COVID-19 prediction model but was indicated as an uncertain parameter in previous modelling studies due to insufficient experimental data in real sewer conditions[2,7,24]. Assuming this degradation rate is correlated with biofilm A/V ratios, it could be estimated that in typical sewage networks with A/V ratio of 10–30 m^{-2} m^{-3} (ref. [25]), approximately 3–18% of RNA GC will degrade in wastewater over an HRT of 2–8 h from releasing points to a WWTP. This hence indicates that uncertainty of RNA decay in the forecast of COVID-19 cases could be relatively small, which prevents substantial underestimation due to RNA GC in-sewer loss. Additionally, the information on RNA in-sewer decay is critical to the low-case settings, particularly those with long HRTs before sample collection. The application of wastewater surveillance in low-case settings showcases its most important benefit during the COVID-19 pandemic, namely providing an early warning tool to effectively identify emergence of SARS-CoV-2 and appearance of new variants in communities[3,19]. This unique feature depends on the sensitivity of the whole wastewater surveillance approach to detect SARS-CoV-2 RNA signals in collected samples. In low-case settings where the overall RNA discharged load is at a low level, in-sewer degradation of RNA could drive the signals below limits of detection or quantification, and consequently diminish the early warning capability. This impact could be enhanced in those low-case settings with long HRTs, such as aircraft wastewater tanks[26], onsite wastewater collection tanks (for example, at hospitals)[27] and scattered communities living far from a WWTP where sewage could be retained in sewer systems (for example, pump stations) for a long period. RNA decay in those long-HRT settings could affect the reverse transcriptase-quantitative polymerase chain reaction (RT–qPCR) detection and quantification results, with the risk of RNA loss below the detection limits and potential for false negatives. For instance, the monitoring of SARS-CoV-2 RNA in long-HRT tanks at a hospital indicated that RNA already largely degraded before sample collection, resulting in a minimum infection rate of 253 cases per 10,000 persons for a positive detection compared with much higher sensitivities (for example, 2 per 10,000) in previous wastewater surveillance[19,27].

The role of sewer biofilms as a reservoir for virus/viral RNA could contribute to prolonged virus presence in wastewater beyond local outbreaks and affect epidemiological inferences based on wastewater surveillance. This becomes more important with the cessation of mass clinical testing and the huge reduction of available clinical data, while wastewater testing can still be applied to provide near real-time health information at the population level and inform public health decision making. Therefore, factors that could affect occurrence and concentrations of SARS-CoV-2 RNA signals in wastewater should be considered, particularly when assessing infection dynamics in low-case settings and/or near the end of an outbreak. In our study, the prolonged persistence and resurgence of SARS-CoV-2 RNA in the Reactor under hydraulic changes corroborated the role of biofilms in protecting viruses from being washed out and releasing partial viral RNA to wastewater. When the Reactor was replaced with new virus-free wastewater, an increasing N_{ww} was unexpectedly observed in the effluent compared with the original GC in the Reactor (considering viruses do not multiply outside their host cell). This was attributed to the enhanced sloughing of virus-bound biofilm particles and pieces during a rapid hydraulic change, as evidenced by an increasing SS concentration in effluent (13.0 mg ml^{-1}) compared with that inside the Reactor before the pumping event (3.9 mg ml^{-1}). Similarly, a previous study detected F-specific RNA bacteriophage immobilized in biofilms while virus signals in wastewater were reduced to below the limit of detection[11]. In a washout study, the decrease of caliciviruses in reactor effluent was slower than predicted due to the role of biofilms in trapping and releasing viruses under high-shear turbulent-flow conditions[13]. Another study found that infectious poliovirus and coliphages in water were reduced below the detection limit after water exchange, but were detectable again a few days later due to transfer of infectious viruses from biofilms to the water phase[12]. A recent study reported the continuous detection of SARS-CoV-2 RNA at hospital sewage for 15 days and in WWTPs for more than 19 days after the end of a local COVID-19 pandemic event, suggesting sewer sediments could be potential virus repositories where the release of viruses caused a longer persistence of SARS-CoV-2 RNA in sewage systems[28]. The issue of persistent SARS-CoV-2 RNA occurrence in sewer systems may coincide with the prolonged faecal shedding after clinical recovery (which could last for weeks despite suggested low prevalence[29,30]), leading to misinterpretation of wastewater surveillance when there were no new confirmed cases reported[28]. This suggests that sewer pipes located downstream of COVID-19 facilities, such as hospitals and quarantine centres previously or currently in use, could form virus reservoirs that have accumulated abundant SARS-CoV-2 genomic fragments; the desorption and release of RNA from these sites could contribute positive signals in wastewater

https://doi.org/10.1038/s44221-023-00033-4

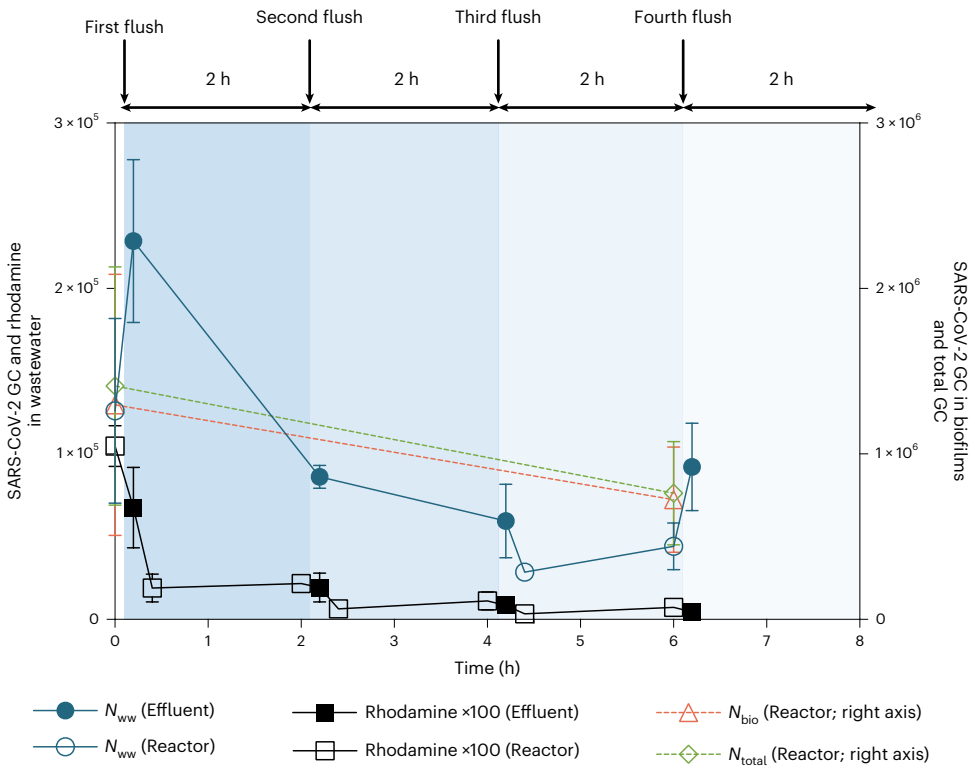

Fig. 4 | Persistence of SARS-CoV-2 RNA under hydraulic changes. Changes of SARS-CoV-2 RNA GC during four flushing events with virus-free wastewater, including RNA GC in wastewater inside the Reactor (N_{ww} $n = 3$, independent samples; blue unfilled circles) and in Reactor effluent (N_{ww} $n = 10$, independent samples; blue filled circles), RNA GC in biofilms of the Reactor (N_{bio} $n = 4$, independent samples; orange unfilled triangles) and the total RNA GC in the Reactor (N_{total} $n = 4$, independent samples; green unfilled diamonds). Data are presented as mean values with s.d. Concurrent rhodamine signals (mV ×100) inside the Reactor ($n = 10$, independent samples; black unfilled squares) and in Reactor effluents ($n = 10$, independent samples; black filled squares) are presented as mean values with s.d. Each blue background sector indicates a 2-h HRT in the Reactor and the blue colour turns lighter when the Reactor experiences more flushing events. Data are provided in source data.

while there is no virus circulating in surrounding areas, which hence misleads health response and interventions. To better understand the prevalence of COVID-19, particularly near or beyond the end of local epidemics, wastewater monitoring at WWTPs and upstream residential subcatchments will provide important complementary information for public health surveillance to differentiate sources of SARS-CoV-2 with higher confidence. Last but not least, we suggest that the findings of this study will be applicable for future studies applying wastewater analysis for surveillance of other infectious diseases.

Methods

Laboratory sewer reactor

A laboratory-scale sewer reactor (the Reactor) was used in this study, which has a demonstrated ability to simulate real sewer conditions (Fig. 1a; for the Reactor images, see Supplementary Fig. 1) (ref. [20]). The Reactor received daily feedings of raw wastewater that was collected every 2 weeks from a sewer pump station in a residential area (experiments were conducted within the week of collection of fresh wastewater). This was typical domestic wastewater characterized as pH 7.5, low sulfide (<3 mg l^{-1}), 10–30 mg l^{-1} sulfate, 180–200 mg l^{-1} soluble chemical oxygen demand, 200–400 mg l^{-1} total suspended solids and 180–380 mg l^{-1} volatile suspended solids. The sewage was stored at 4 °C and warmed to room temperature through a water bath before entering the Reactor. The Reactor contained 750 ml of wastewater and a small buffer container over the lid, which contained 70 ml of wastewater to ensure the inner reactor was completely filled and under the anaerobic condition of rising main sewer. The inner reactor surface area for biofilm development was 425 cm^2. Additionally, removable biofilm carriers (K1 size filter media; surface area of 4.5 cm^2 for each) were installed in the Reactor to allow biofilm growth for at least 3 months before the experiment, which developed the same biofilms as those on the Reactor inner surface. These removable biofilm carriers were used for the analysis and quantification of SARS-CoV-2 RNA in the biofilm phase, while the intact biofilm system on the Reactor inner surface remained unaffected. To simulate the plug-flow condition in real rising mains, the Reactor was subjected to four wastewater exchange events per day (every 6 h) using a peristaltic pump (Masterflex 7520-47, Cole Parmer). Each wastewater exchange event lasted 2 min, during which new wastewater (750 ml) was introduced through the Reactor inlet, with the same volume of wastewater drained through the outlet. Additionally, a magnetic stir provided continuous mixing (250 r.p.m.) inside the Reactor. Before the experiments, background samples for both wastewater and biofilm carriers were taken from the Reactor. The analysis of these background samples indicated that the Reactor had experienced a certain level of SARS-CoV-2 contamination due to daily feeding with real domestic wastewater collected during the COVID-19 prevalence period. For experiments that required the seeding of external SARS-CoV-2 RNA into the Reactor, there was a 3-week interval between duplicate or triplicate batch tests to prevent cross contamination, during which the Reactor was operated under normal conditions with daily pumping events. No additional disinfection or decontamination process was undertaken to avoid impacting sewer biofilms.

Sources of SARS-CoV-2 RNA

Two types of SARS-CoV-2 were used in this study. One was a working stock of gamma-irradiated SARS-CoV-2 (hCoV-19/Australia/

VIC01/2020) that was used for method development, quality control[31] and the sorption experiment. The other was untreated wastewater containing endogenous SARS-CoV-2 collected from WWTPs no more than 1 week before the experiments. During this study, there was a high prevalence of COVID-19 infection in the study area (daily new cases of 1,000–16,000 among the total population of 5.18 million in Queensland, Australia, January to March 2022), leading to high concentrations of endogenous SARS-CoV-2 RNA in untreated wastewater (7.1×10^4 to 5.9×10^5 GC l^{-1}). Additionally, a batch of untreated (archived) wastewater samples that were RT–PCR negative for SARS-CoV-2 was used as the negative control (that is, the virus-free wastewater) in the flushing experiment.

Sorption experiment

We assessed the sorption behaviour of SARS-CoV-2 to the solid compartments in sewers, including SS and biofilms. The sorption equilibrium was performed inside the Reactor and in the Chambers that represented conditions outside the Reactor. The major difference between the Reactor and the Chamber was the abundance of biofilms. Each Chamber contained 50 ml wastewater seeded with gamma-irradiated SARS-CoV-2 at selected concentrations (5.6×10^2 to 7.9×10^5 GC l^{-1}; Supplementary Table 1) across five batch tests, with one to two biofilm carriers transferred from the Reactor to each Chamber right before each batch test. After a contact time of at least 24 h, biofilm carriers were lifted from the Chamber, gently shaken to remove excess water and placed in a separate sterile vial. The wastewater remaining in the Chamber was transferred to a sterile Falcon tube (50 ml) and centrifuged (4,500*g* for 30 min) to separate SS from liquid. To evaluate RNA sorption behaviour in the Reactor, paired wastewater and biofilm samples were taken from individual batch tests where the Reactor was seeded with endogenous SARS-CoV-2 at different concentrations (Supplementary Table 1). After a retention time of 4–24 h, paired wastewater samples (20–50 ml) and biofilm carriers (one to two units) were taken from the Reactor and transferred to separate sterile vials. Wastewater was immediately centrifuged to separate SS from liquid. The biofilm carrier treatment and wastewater centrifugation methods were the same as described for the tests in the Chambers.

In-sewer SARS-CoV-2 RNA decay experiment

Triplicate batch tests were conducted to investigate the decay of SARS-CoV-2 RNA in a realistic sewer environment under the impact of biofilms. At the beginning of a batch test, wastewater (1,000 ml) with known endogenous SARS-CoV-2 was pumped into the Reactor. After a rapid mixing, wastewater samples (20 ml each) were collected at 0, 2, 4, 6 and 24 h from the Reactor. Samples of biofilm carriers were taken right before the pumping event (time 0) and immediately after wastewater sample collection at 24 h. This was intended to avoid impact on the anaerobic condition in the Reactor during the experimental period. Biological activities in the Reactor were monitored by measuring sulfur species in the first hour after the wastewater feeding. Samples for sulfur species analysis were preserved using a solution of sulfide antioxidant buffer and analysed by an ion chromatograph with an ultraviolet and conductivity detector (Dionex ICS-2000). At the beginning of a batch test, rhodamine was added into the feeding wastewater at 200 μg l^{-1} as a water tracer to indicate real-time hydraulic dynamics in the Reactor. Rhodamine concentrations were measured by a portable Cyclops-7 Submersible Rhodamine Sensor coupled with a Cyclops Explorer[20].

Flushing experiment

Flushing experiments (performed in duplicate) were conducted to evaluate the persistence of SARS-CoV-2 RNA in the Reactor under the impact of wastewater exchanges, which simulated the plug-flow condition in real sewer pipes. Immediately following the in-sewer decay experiments where sewer biofilms had been in contact with SARS-CoV-2 RNA for 24 h, 1 l of virus-free wastewater (negative for SARS-CoV-2) was pumped into the Reactor. This pumping event caused wastewater exchange, displacing a majority of the existing wastewater (SARS-CoV-2 positive) in the Reactor. During a batch test, four wastewater exchange events were triggered every 2 h, that is, at 0.1, 2.1, 4.1 and 6.1 h. Wastewater samples (50 ml each) were collected from the Reactor before or after each wastewater exchange event as well as from the Reactor effluents after each wastewater exchange. Biofilm carriers were taken from the Reactor after the fourth exchange event (at 6.2 h). Rhodamine signals were measured in the Reactor and effluents throughout the batch tests.

Sample processing, virus RNA concentration and extraction

The collected samples, including the already centrifuged samples for liquid and SS separation, samples of wastewater mixture and biofilm carrier samples, were processed separately by filtration using electronegative membranes (MF-Millipore, pore size 0.45 μm, diameter 47 mm; HAWP04700; Merck Millipore Ltd.). For the centrifuged samples, the supernatant was directly filtered through the electronegative membranes, and the settled solids were mixed with phosphate-buffered saline (PBS) (0.2–0.8 ml, depending on the amount of settled solids) and then filtered through the electronegative membranes. The mass of SS in each sample was measured by the weights of a Falcon tube (50 ml) before and after SS transfer. For measuring the combined viral GC in the wastewater mixture, wastewater samples (containing liquid and SS) were directly filtered through the membranes. For the biofilm carriers in each sterile vial, PBS (1–2 ml, depending on the number of biofilm carriers collected) was added and the vial was vortexed to enhance biofilm sloughing from the carriers. Biofilms were also scraped from the carrier using a small sterile brush when necessary. The mixture of suspended biofilms and PBS was filtered through the electronegative membranes.

After filtration, electronegative membranes were folded and immediately inserted into individual 5 ml bead-beating tubes (Qiagen) using sterile forceps for nucleic acid extraction. Nucleic acid was extracted directly from the electronegative membranes using the RNeasy PowerWater Kit (cat. no. 14700-50-NF) (Qiagen). Before homogenization, 990 μl of buffer PM1 and 10 μl of β-mercaptoethanol (Sigma-Aldrich; M6250-10 ml) were added into each bead-beating tube. The bead-beating tubes were then homogenized using a Precellys 24 tissue homogenizer (Bertin Technologies) set for 3 × 15 s at 10,000 r.p.m. at a 10 s interval. After homogenization, the tubes were centrifuged at 4,000*g* for 5 min to pellet the filter debris and beads. Sample lysate supernatant ranging from 600 μl to 800 μl in volume was then used to extract nucleic acid following the manufacturer's specified protocol. One minor modification was made: the use of DNase I solution was omitted from the protocol to isolate nucleic acid (that is, both RNA and DNA).

PCR inhibition

The presence of PCR inhibition in the nucleic acid sample was assessed using the semi-quantitative murine hepatitis virus (MHV) RT–PCR assay[32] after seeding approximately 10^3 gene copy MHV/RT–PCR reaction with wastewater nucleic acid samples. The MHV stock was prepared in a previous study using 20 faecal samples of naturally infected mice collected from a snake farm[18]. To determine PCR inhibition, identical concentrations of MHV (10^3 gene copy) were also added to the PCR reaction without the wastewater nucleic acid sample and the mean Cq value was used to establish a reference point. All samples were analysed alongside three no template controls. If the Cq value of the nucleic acid sample was >2 Cq values compared with the reference Cq values, the sample was considered to have PCR inhibitors[33].

RT–dPCR analysis

The optimized United States Centers for Disease Control and Prevention (US CDC) N1 assay was performed in 40 μl reaction mixtures using the QIAcuity One-Step Viral RT–PCR Kit (cat. no. 1123145, Qiagen) and 26,000 24-well Nanoplates (cat. no. 250001, Qiagen)[34]. The US CDC

N1 RT digital PCR (RT–dPCR) mixture contained 10 µl of master mix, 800 nM forward primer, 800 nM reverse primer, 200 nM probe, 0.4 µl of 100× Multiplex Reverse Transcription Mix, 19.2 µl of DNase- and RNase-free water, and 5 µl of template RNA. Two RT–dPCR replicates were used for each sample. The 40 µl RT–dPCRs were prepared in a 96-well preplate and then transferred into the 26,000 24-well Nanoplates. The nanoplate was then loaded onto the QIAcuity dPCR 5-plex platform (Qiagen) and subject to an automated workflow that included (1) a priming and rolling step to generate and isolate the chamber partitions, (2) an amplification step using the thermal cycling protocol (50 °C for 40 min for reverse transcription, 95 °C for 2 min for enzyme activation, 95 °C for 5 s for denaturation and 60 °C for 90 s for annealing/extension for 45 cycles) and (3) a final imaging step made by reading in the FAM channel. The experiments were performed using duplicate RT–dPCR-negative and RT–dPCR-positive (γ-irradiated SARS-CoV-2 RNA) controls. To minimize RT–dPCR contamination, RNA extraction and RT–dPCR setup were performed in separate laboratories. The US CDC N1 RT–dPCR assay limit of detection (ALOD) has been reported in a recent study[34]. The ALOD was defined by fitting a cumulative Gaussian distribution to the observed proportion of positive technical replicates along the dilution series. The 95% ALOD was estimated as the 95th percentile of the resulting normal distribution.

Quality control and RT–dPCR data analysis

Data were analysed using the QIAcuity Suite Software version 1.1.3 193 (Qiagen), and quantities expressed as GC per microlitre of reaction mixture. The RT–dPCR assays were performed using automatic settings for the threshold and baseline. For RT–dPCR, samples were considered positive if there were at least two positive partitions following the merging of two replicate wells. Samples were considered quantifiable by RT–dPCR if the concentrations were above the ALOD, and the average number of partitions was >15,000. Samples were considered negative (<ALOD) when no amplification was observed in any of the partitions and the RT–dPCR negative controls were negative. For all samples collected in this study, the RT–dPCR results were positive and quantifiable.

Assay performance characteristics and QA/QC

All nucleic acid samples were within the 2-Cq values of the reference Cq value; thus, no qPCR inhibition was identified. All RT–PCR and RT–dPCR negative controls were negative and positive controls amplified in each PCR run. For US CDC N1 RT–dPCR, the number of partitions ranged from 15,213 to 24,312 with a mean ± s.d. of 22,355 ± 1,987. The US CDC N1 RT–dPCR ALOD was 2.9 GC/reaction[34].

Data analysis and kinetics evaluation

Concentrations of SARS-CoV-2 RNA were determined by the detected GC numbers in a sample and its corresponding mass, volume or surface area. Viral RNA concentrations in different sewage compartments, namely wastewater mixture (C_{ww}, GC ml^{-1}), wastewater liquid (C_l, GC ml^{-1}), suspended solids (C_{ss}, GC g^{-1}) and sewer biofilms (C_{bio}, GC cm^{-2}), were calculated. The total number of SARS-CoV-2 RNA in the reactor (N_{total}) comprised the number of RNA GC in wastewater (N_{ww} = reactor volume × C_{ww}) and the number of RNA GC in biofilms (N_{bio} = reactor inner surface area × C_{bio}). Sorption coefficients of SARS-CoV-2 RNA between liquid and SS (K_{d_ss}, ml g^{-1}) and between wastewater mixture and sewer biofilms (K_{d_bio}, ml cm^{-2}) were estimated by equations (1) and (2), respectively. A larger value of K_d indicates the greater adsorption tendency.

$$C_{ss} = K_{d\_ss} \times C_l \quad (1)$$

$$C_{bio} = K_{d\_bio} \times C_{ww} \quad (2)$$

The decrease in SARS-CoV-2 RNA concentrations (k_1, h^{-1}) and the changes in numbers of GC in the Reactor (k_2, h^{-1}) were described by the first-order kinetics (equations (3) and (4)). First-order kinetics was selected due to its better data fitting performance compared with linear regression, two-phase decay and second-order kinetics (Table 2). In this study, k represented a combined result of all biotic and abiotic in-sewer processes that could be related to virus transformation, including sorption and biodegradation. Half-lives (T_{50}) and the time to 90% change (T_{90}) were estimated by equations (5) and (6), respectively. The estimation of modelling parameters was performed in RStudio (v 1.3.959).

$$C = C_0 \times e^{-k_1 \times t} \quad (3)$$

$$N = N_0 \times e^{-k_2 \times t} \quad (4)$$

$$T_{50} = \ln(0.5)/k \quad (5)$$

$$T_{90} = \ln(0.1)/k \quad (6)$$

Reporting summary

Further information on research design is available in the Nature Portfolio Reporting Summary linked to this article.

Data availability

Data obtained and used during the current study are provided in Supplementary Information. Source data are provided with this paper.

References

1. Wu, F. et al. SARS-CoV-2 RNA concentrations in wastewater foreshadow dynamics and clinical presentation of new COVID-19 cases. *Sci. Total Environ.* **805**, 150121 (2022).
2. Weidhaas, J. et al. Correlation of SARS-CoV-2 RNA in wastewater with COVID-19 disease burden in sewersheds. *Sci. Total Environ.* **775**, 145790 (2021).
3. Karthikeyan, S. et al. Wastewater sequencing reveals early cryptic SARS-CoV-2 variant transmission. *Nature* **609**, 101–108 (2022).
4. Ahmed, W. et al. First confirmed detection of SARS-CoV-2 in untreated wastewater in Australia: a proof of concept for the wastewater surveillance of COVID-19 in the community. *Sci. Total Environ.* **728**, 138764 (2020).
5. Medema, G., Heijnen, L., Elsinga, G., Italiaander, R. & Brouwer, A. Presence of SARS-coronavirus-2 RNA in sewage and correlation with reported COVID-19 prevalence in the early stage of the epidemic in The Netherlands. *Environ. Sci. Tech. Lett.* **7**, 511–516 (2020).
6. Ahmed, W. et al. Minimizing errors in RT-PCR detection and quantification of SARS-CoV-2 RNA for wastewater surveillance. *Sci. Total Environ.* **805**, 149877 (2022).
7. Li, X., Zhang, S., Shi, J., Luby, S. P. & Jiang, G. Uncertainties in estimating SARS-CoV-2 prevalence by wastewater-based epidemiology. *Chem. Eng. J.* **415**, 129039 (2021).
8. Skraber, S. et al. Occurrence and persistence of bacterial and viral faecal indicators in wastewater biofilms. *Water Sci. Technol.* **55**, 377–385 (2007).
9. Storey, M. V. & Ashbolt, N. J. Persistence of two model enteric viruses (B40-8 and MS-2 bacteriophages) in water distribution pipe biofilms. *Water Sci. Technol.* **43**, 133–138 (2001).
10. Pelleieux, S. et al. Accumulation of MS2, GA, and Qbeta phages on high density polyethylene (HDPE) and drinking water biofilms under flow/non-flow conditions. *Water Res.* **46**, 6574–6584 (2012).
11. Skraber, S. et al. Occurrence and persistence of enteroviruses, noroviruses and F-specific RNA phages in natural wastewater biofilms. *Water Res.* **43**, 4780–4789 (2009).

12. Helmi, K. et al. Interactions of *Cryptosporidium parvum*, *Giardia lamblia*, vaccinal poliovirus type 1, and bacteriophages phiX174 and MS2 with a drinking water biofilm and a wastewater biofilm. *Appl. Environ. Microbiol.* **74**, 2079–2088 (2008).
13. Lehtola, M. J. et al. Survival of *Mycobacterium avium*, *Legionella pneumophila*, *Escherichia coli*, and caliciviruses in drinking water-associated biofilms grown under high-shear turbulent flow. *Appl. Environ. Microbiol.* **73**, 2854–2859 (2007).
14. Skraber, S., Schijven, J., Gantzer, C. & Husman, A. D. R. Pathogenic viruses in drinking-water biofilms—a public health risk? *Biofilms* **2**, 105 (2005).
15. Gundy, P. M., Gerba, C. P. & Pepper, I. L. Survival of coronaviruses in water and wastewater. *Food Environ. Virol.* **1**, 10–14 (2009).
16. Bivins, A. et al. Persistence of SARS-CoV-2 in water and wastewater. *Environ. Sci. Tech. Lett.* **7**, 937–942 (2020).
17. Shi, J. et al. Enhanced decay of coronaviruses in sewers with domestic wastewater. *Sci. Total Environ.* **813**, 151919 (2022).
18. Ahmed, W. et al. Decay of SARS-CoV-2 and surrogate murine hepatitis virus RNA in untreated wastewater to inform application in wastewater-based epidemiology. *Environ. Res.* **191**, 110092 (2020).
19. Li, J. et al. Monitoring of SARS-CoV-2 in sewersheds with low COVID-19 cases using a passive sampling technique. *Water Res.* **218**, 118481 (2022).
20. Li, J. et al. Stability of illicit drugs as biomarkers in sewers: from lab to reality. *Environ. Sci. Technol.* **52**, 1561–1570 (2018).
21. Helmi, K. et al. Adenovirus, MS2 and PhiX174 interactions with drinking water biofilms developed on PVC, cement and cast iron. *Water Sci. Technol.* **61**, 3198–3207 (2010).
22. Li, B., Di, D. Y. W., Saingam, P., Jeon, M. K. & Yan, T. Fine-scale temporal dynamics of SARS-CoV-2 RNA abundance in wastewater during A COVID-19 lockdown. *Water Res.* **197**, 117093 (2021).
23. Graham, K. E. et al. SARS-CoV-2 RNA in wastewater settled solids is associated with COVID-19 cases in a large urban sewershed. *Environ. Sci. Technol.* **55**, 488–498 (2021).
24. Kantor, R. S., Nelson, K. L., Greenwald, H. D. & Kennedy, L. C. Challenges in measuring the recovery of SARS-CoV-2 from wastewater. *Environ. Sci. Technol.* **55**, 3514–3519 (2021).
25. McCall, A. K., Palmitessa, R., Blumensaat, F., Morgenroth, E. & Ort, C. Modeling in-sewer transformations at catchment scale—implications on drug consumption estimates in wastewater-based epidemiology. *Water Res.* **122**, 655–668 (2017).
26. Jones, D. L. et al. Suitability of aircraft wastewater for pathogen detection and public health surveillance. *Sci. Total Environ.* **856**, 159162 (2022).
27. Hong, P. Y. et al. Estimating the minimum number of SARS-CoV-2 infected cases needed to detect viral RNA in wastewater: to what extent of the outbreak can surveillance of wastewater tell us? *Environ. Res.* **195**, 110748 (2021).
28. Yang, S. et al. Persistence of SARS-CoV-2 RNA in wastewater after the end of the COVID-19 epidemics. *J. Hazard. Mater.* **429**, 128358 (2022).
29. Jones, D. L. et al. Shedding of SARS-CoV-2 in feces and urine and its potential role in person-to-person transmission and the environment-based spread of COVID-19. *Sci. Total Environ.* **749**, 141364 (2020).
30. Li, X. et al. SARS-CoV-2 shedding sources in wastewater and implications for wastewater-based epidemiology. *J. Hazard. Mater.* **432**, 128667 (2022).
31. Ahmed, W. et al. Evaluation of process limit of detection and quantification variation of SARS-CoV-2 RT-qPCR and RT-dPCR assays for wastewater surveillance. *Water Res.* **213**, 118132 (2022).
32. Besselsen, D. G., Wagner, A. M. & Loganbill, J. K. Detection of rodent coronaviruses by use of fluorogenic reverse transcriptase-polymerase chain reaction analysis. *Comparative Med.* **52**, 111–116 (2002).
33. Staley, C., Gordon, K. V., Schoen, M. E. & Harwood, V. J. Performance of two quantitative PCR methods for microbial source tracking of human sewage and implications for microbial risk assessment in recreational waters. *Appl. Environ. Microbiol.* **78**, 7317–7326 (2012).
34. Ahmed, W. et al. Comparison of RT-qPCR and RT-dPCR platforms for the trace detection of SARS-CoV-2 RNA in wastewater. *ACS ES T Water* **2**, 1871–1880 (2022).

Acknowledgements

This study was supported by Queensland Health (Australia) as a part of Queensland's wastewater surveillance programme for SARS-CoV-2. P.K.T. acknowledges an Australian Research Council (ARC) Discovery project (DP220101790).

Author contributions

J.L., W.A., S.L.S., K.V.T., J.F.M. and P.K.T. conceived and designed the experiments. S.L.S. and J.F.M. supervised the study. J.L. performed experiments. W.A., S.M., W.J.M.S., X.C. and M.Z. contributed materials and analysis tools. W.A., S.M. and W.J.M.S. performed sample analysis of SARS-CoV-2 RNA. J.L. and W.A. performed data analysis and interpretation. J.L. and W.A. wrote the original and revised the manuscript drafts. All authors contributed to reviewing and editing of the manuscript.

Competing interests

The authors declare no competing interests.

Additional information

Supplementary information The online version contains supplementary material available at https://doi.org/10.1038/s44221-023-00033-4.

Correspondence and requests for materials should be addressed to Jiaying Li.

Peer review information *Nature Water* thanks Manish Kumar and the other, anonymous, reviewer(s) for their contribution to the peer review of this work.

nature portfolio

Corresponding author(s): Jiaying Li

Last updated by author(s): Jan 6, 2023

Reporting Summary

Nature Portfolio wishes to improve the reproducibility of the work that we publish. This form provides structure for consistency and transparency in reporting. For further information on Nature Portfolio policies, see our Editorial Policies and the Editorial Policy Checklist.

Statistics

For all statistical analyses, confirm that the following items are present in the figure legend, table legend, main text, or Methods section.

n/a	Confirmed
☐	☒ The exact sample size (*n*) for each experimental group/condition, given as a discrete number and unit of measurement
☐	☒ A statement on whether measurements were taken from distinct samples or whether the same sample was measured repeatedly
☐	☒ The statistical test(s) used AND whether they are one- or two-sided *Only common tests should be described solely by name; describe more complex techniques in the Methods section.*
☐	☒ A description of all covariates tested
☒	☐ A description of any assumptions or corrections, such as tests of normality and adjustment for multiple comparisons
☐	☒ A full description of the statistical parameters including central tendency (e.g. means) or other basic estimates (e.g. regression coefficient) AND variation (e.g. standard deviation) or associated estimates of uncertainty (e.g. confidence intervals)
☐	☒ For null hypothesis testing, the test statistic (e.g. *F*, *t*, *r*) with confidence intervals, effect sizes, degrees of freedom and *P* value noted *Give P values as exact values whenever suitable.*
☒	☐ For Bayesian analysis, information on the choice of priors and Markov chain Monte Carlo settings
☒	☐ For hierarchical and complex designs, identification of the appropriate level for tests and full reporting of outcomes
☒	☐ Estimates of effect sizes (e.g. Cohen's *d*, Pearson's *r*), indicating how they were calculated

Our web collection on statistics for biologists contains articles on many of the points above.

Software and code

Policy information about availability of computer code

Data collection	GraphPad Prism 8 was used to collect and organize experimental data.
Data analysis	GraphPad Prism 8 was used for statistical analysis and data visualization. RStudio (v 1.3.959) was used for modeling and statistical analysis. RT-dPCR data were analysed using the QIAcuity Suite Software version 1.1.3 193 (Qiagen).

For manuscripts utilizing custom algorithms or software that are central to the research but not yet described in published literature, software must be made available to editors and reviewers. We strongly encourage code deposition in a community repository (e.g. GitHub). See the Nature Portfolio guidelines for submitting code & software for further information.

Data

Policy information about availability of data

All manuscripts must include a data availability statement. This statement should provide the following information, where applicable:

- Accession codes, unique identifiers, or web links for publicly available datasets
- A description of any restrictions on data availability
- For clinical datasets or third party data, please ensure that the statement adheres to our policy

Data obtained and used during the current study are provided in Supplementary Information, Source data file and available in public data repository.

Human research participants

Policy information about studies involving human research participants and Sex and Gender in Research.

Reporting on sex and gender	Sex/gender-based data were not considered in this study design.
Population characteristics	N.A.
Recruitment	N.A.
Ethics oversight	N.A.

Note that full information on the approval of the study protocol must also be provided in the manuscript.

Field-specific reporting

Please select the one below that is the best fit for your research. If you are not sure, read the appropriate sections before making your selection.

☐ Life sciences ☐ Behavioural & social sciences ☒ Ecological, evolutionary & environmental sciences

For a reference copy of the document with all sections, see nature.com/documents/nr-reporting-summary-flat.pdf

Ecological, evolutionary & environmental sciences study design

All studies must disclose on these points even when the disclosure is negative.

Study description

The study aimed to understand the fate of SARS-CoV-2 in sewer systems to improve the application of wastewater surveillance for monitoring and management of the COVID-19 pandemic. A laboratory sewer biofilm reactor was employed to investigate sorption, decay, and persistence of SARS-CoV-2 RNA in sewers under various realistic hydraulic conditions. Findings of this study will help enhancing the ability of wastewater surveillance to assess COVID-19 prevalence in the population and complement public health systems, especially at low infection-case settings and when mass clinical testing has been reduced.

Research sample

Samples were taken from the sewer biofilm reactor and testing chambers during three main experiments, namely the Sorption experiment (18 independent batch tests), the Decay experiment (triplicate batch tests), and the Flushing experiment (duplicate batch tests). Untreated wastewater with known numbers of endogenous SARS-CoV-2 and the working solution of gamma-inactivated SARS-CoV-2 were used during this study as external sources of SARS-CoV-2 RNA GC. Specifically, untreated wastewater containing endogenous SARS-CoV-2 was collected from local wastewater treatment plants no more than 1 week before each experiment. During this study, there was a high prevalence of COVID-19 infection in the study area (daily new cases of 1,000 - 16,000 among the total population of 5.18 million in Queensland, Australia, January to March 2022), leading to high concentrations of endogenous SARS-CoV-2 RNA in untreated wastewater.

During the experiments, at each sampling point, a set of samples were collected from different sewer compartments, namely wastewater mixture, wastewater liquid, suspended solids, and/or sewer biofilms. Each sample was processed and analyzed using RT-dPCR (US CDC N1 assay). Additionally, during the Sorption and the Flushing experiments, rhodamine was added together with external SARS-CoV-2 sources as a water tracer to indicate real-time hydraulic dynamics in the Reactor, of which the signals were measured using an online sensor.

Sampling strategy

The Sorption experiment was designed to investigate the sorption potentials of SARS-CoV-2 RNA to solid compartments in sewers and determine sorption coefficients. Two sewer settings were used, namely the sewer biofilm reactor (Reactor) and the testing chambers (Chambers), to provide the sewer conditions with different abundance of biofilms. Known numbers of SARS-CoV-2 RNA GC were added into the Reactor and Chambers to create the sewage conditions with a range of environmentally-relevant RNA concentrations from low to high levels (statistically significantly different, $p < 0.05$) across different batch tests. Samples were taken from different sewer compartments during each batch test.

The Decay experiment was designed to investigate the stability of SARS-CoV-2 RNA in sewers under the influence of biofilms. At the beginning of a batch test, wastewater with known endogenous SARS-CoV-2 was pumped into the Reactor, and samples were collected during the subsequent 24-h HRTs. The maximal number of wastewater samples (20-mL each) that could be taken from the reactor was determined by the volume of the buffer container (70-mL) and connecting tubes of the Reactor to avoid excessive sampling of wastewater and hence affecting the anaerobic condition inside the Reactor.

The Persistence experiment was designed to investigate the role of biofilms in entrapping and further distributing virus particles under hydraulic changes. This experiment was conducted immediately following the Decay experiments where sewer biofilms had been in contact with SARS-CoV-2 RNA for 24 h. During a batch test, four flushing events using virus-free wastewater (negative for SARS-CoV-2) were triggered intermittently (every 2 h) to simulate the plug-flow condition in real sewer pipes and to flush the original SARS-CoV-2 positive wastewater away from the Reactor. Wastewater samples were collected from inner Reactor and the Reactor effluent before and after each wastewater exchange event. Biofilm carriers were taken from the Reactor after the last exchange event.

Data collection	Sampling information was recorded during the experiments. Samples were processed and analysed using RT-dPCR and data were analysed using the QIAcuity Suite Software version 1.1.3 193 (Qiagen). Data of SARS-CoV-2 RNA GC for individual samples and the corresponding sampling time, volume, mass, or surface area of corresponding matrix, and sampling locations were integrated in Microsoft Excel and GraphPad Prism 9.
Timing and spatial scale	In Sorption experiment, samples were taken from different sewer compartments after a contact time of 4 - 24 h with seeded SARS-CoV-2 RNA. This contact time represented hydraulic retention times (HRTs) in real sewers ranging from normal to extremely long periods. In Decay experiment, wastewater samples were collected at 0, 2, 4, 6, and 24 h from the Reactor. Sampling time points were selected based on previous experiences in sewer transformation study and the maximum numbers of samples that could be taken from the Reactor without affecting the anaerobic condition. This 24-h sampling period was able to cover a broad time window of HRTs in real sewer systems. Samples of biofilm carriers were taken right before the pumping event (time 0) and immediately after wastewater sample collection at 24 h. This was intended to avoid impact on the anaerobic condition in the Reactor during the experimental period. In Flushing experiment, four wastewater-exchange events were triggered every 2 h, i.e., at 0.1, 2.1, 4.1 and 6.1 h, which represented a typical HRT of 2 h in real rising main pipe. Wastewater samples were collected from the Reactor effluents after each wastewater exchange (at 0.2, 2.2, 4.2, and 6.2 h) and from the Reactor before or after wastewater exchange events (at 0, 4.4, and 6 h) to determine the level of SARS-CoV-2 RNA remained in the sewer section. Biofilm carriers were taken from the Reactor after the 4th exchange event (at 6.2 h) to avoid impact on the anaerobic condition in the Reactor during the experimental period. For experiments that required the seeding of external SARS-CoV-2 RNA into the Reactor, there was a three-week interval between duplicate or triplicate batch tests to prevent cross contamination, during which the Reactor was operated under normal condition with daily pumping events.
Data exclusions	All collected samples from various sewage compartments during the experiments had detected and quantifiable RNA. No data were excluded from the analyses.
Reproducibility	In Sorption experiment, a number of independent batch tests (n=18) was conducted to simulate the sewage conditions with a range of environmentally-relevant RNA concentrations from low to high levels. This allowed us to investigate the potential correlation between RNA concentrations in the liquid and solid compartments based on observations from multiple independent batch tests. In Sorption and Flushing experiments, the batch tests were conducted in duplicate or triplicate independently to verify the reproducibility of experimental findings. All attempts to repeat the experiment were successful. For sample analysis, two RT-dPCR replicates were used for each sample, and the experiments were performed using duplicate RT-dPCR negative and positive (γ-irradiated SARS-CoV-2 RNA) controls. To minimize RT-dPCR contamination, RNA extraction and RT-dPCR setup were performed in separate laboratories. For all samples collected in this study, the RT-dPCR results were positive and quantifiable. The presence of PCR inhibition in nucleic acid sample was assessed using the semi-quantitative murine hepatitis virus (MHV) RT-PCR assay (see Methods for details). All samples were analyzed alongside three no template controls. All nucleic acid samples were within the 2-Cq values of the reference Cq value; thus, no qPCR inhibition was identified. All RT-PCR and RT-dPCR negative controls were negative and positive controls amplified in each PCR run.
Randomization	During the entire study, samples were allocated into four groups representing different sewer compartments, namely the groups of samples collected from wastewater mixture, wastewater liquid, suspended solids, and sewer biofilms. In the Sorption experiment, samples were additionally allocated to two groups representing different sewer settings, namely the groups of samples from the Reactor and the Chambers.
Blinding	Blinding was not applicable to this study as there was no experiments involving specific treatments or groups.

Did the study involve field work? ☐ Yes ☒ No

Reporting for specific materials, systems and methods

We require information from authors about some types of materials, experimental systems and methods used in many studies. Here, indicate whether each material, system or method listed is relevant to your study. If you are not sure if a list item applies to your research, read the appropriate section before selecting a response.

Materials & experimental systems

n/a	Involved in the study
☒	☐ Antibodies
☒	☐ Eukaryotic cell lines
☒	☐ Palaeontology and archaeology
☒	☐ Animals and other organisms
☒	☐ Clinical data
☒	☐ Dual use research of concern

Methods

n/a	Involved in the study
☒	☐ ChIP-seq
☒	☐ Flow cytometry
☒	☐ MRI-based neuroimaging